European Journal of Control (2007)4:1–21

European Journal of Control

Adaptive and Predictive Path Tracking Control for Off-road Mobile Robots

Roland Lenain[1], Benoit Thuilot[2], Christophe Cariou[1], and Philippe Martinet[2]

[1]Cemagref, 24 av. des Landais BP50085, 63172 Aubière CEDEX, France;
[2]LASMEA, 24 av. des Landais, 63177 Aubière CEDEX, France

A major problem in the design of control laws dedicated to mobile robots appears when the classical hypothesis of rolling without sliding wheels is violated. It is generally the case for off-road vehicles as adherence conditions are often not satisfactory and sliding can then cease to be negligible. Consequently theoretical performance is impaired and the vehicle is no longer accurately controlled.

It is particularly harmful with respect to path tracking tasks, where a loss of accuracy in rough terrain can generate a hazardous situation. Previous work based on the assumption of rolling without sliding has shown very satisfactory results with respect to that task when sliding is not preponderant. It has also made it possible to pinpoint and study the effects of sliding when it appears to be non-negligible.

To preserve path tracking accuracy with respect to this phenomenon, a new control law based on an extended kinematic model (updated on-line via an adaptive method) is proposed and discussed. Such control is very efficient when adherence conditions are constant, but overshoots can appear when an abrupt variation is recorded (which is especially the case at the beginning/end of curves due to low level delays and inertial effects). A model predictive control approach is then added to limit such transient phases in cases where a curved path is followed.

The paper is organized as follows: the extended kinematic model is presented as well as the observation of unmeasured parameters required to feed it. A non-linear control law can then be designed and the results obtained are discussed. Finally, the model predictive control approach is integrated and the overall control scheme is presented. The capabilities of the approach described in this paper are then discussed through full scale experiments.

Keywords: Adaptive control; mobile robots; model predictive control; path tracking; sliding effects

1. Introduction

Automated algorithms dedicated to the control of mobile robots have always been an important issue in robotics with respect to the potential benefits they could bring in numerous fields of everyday life. From the help of indoor robots dedicated to housework, museum or industrial conveying (see for instance [3] and [14]) to vehicle driving assistance (e.g. [28]) or the exploration of hazardous environments (see for instance [20]), many autonomous applications need accurate and efficient navigation systems. Such control algorithms and theoretical principles are closely linked to the application and available sensors. Many different kinds of control strategies have thus been applied and tested for automatic guidance of vehicles.

Some of these approaches are focused on control without models, such as neural network control described for instance by [25] applied to an all-terrain car. However, most control strategies rely on a model,

Correspondence to:

Received 24 August 2005; Accepted 30 October 2006
Recommended by F. Allgower, D. Clarke

particularly the celebrated Ackermann model (the vehicle is viewed as a bicycle) assuming rolling without sliding (RWS). Such a model is used for example for flatness feedback control (detailed in [13] or for chained system control (see [26]), which are particularly convenient for trajectory tracking in the mobile robotics field. If the Ackermann model is sufficient for many applications (especially dealing with indoor mobile robotics), the RWS condition is not always satisfactory, in particular with respect to off-road mobile robots, and leads to inaccurate results (as has been pointed out for instance in [17]). More detailed models are then required, the complexity of which depends on the application (accuracy desired) and on the kind of control expected to be applied.

The integration of sliding effects can be naturally achieved by the use of dynamic models of vehicle and tyre-soil interaction. This is partially done for instance in [11], but applied to road vehicles, using the celebrated Pacejka tyre model. Unfortunately, such models are highly dependent on their parameters which, moreover, vary over time in the case of off-road vehicle control. As a consequence, their on-line estimation appears to be quite unsuitable. Therefore, some control techniques have been investigated to preserve accuracy of control without integrating sliding phenomena into the modelling (such as Sliding Mode Control investigated in [6]). However, they generally appear to be theoretically oscillating and cannot consequently be applied to high accuracy tasks.

This paper addresses the problem of high accuracy lateral path tracking of off-road car-like robots, running on low adherence ground. The objective is to design a control strategy which allows a tracking accuracy of ± 15 cm to be reached, whatever the conditions of adherence and whatever the path to be followed. To obtain such tracking accuracy, an important problem to be taken into account – in addition to the sliding effect – is the inevitable delay between the desired control variable and the actuator response (due to low level settling time). This delay is emphasized when the mobile robot to be controlled is heavy and velocity is important (as vehicle inertia ceases to be negligible). A time-delay system (see [24] for an overview of this kind of system and general possible solutions) must then be considered to prevent lapses in path tracking accuracy from overshoots appearing at each abrupt variation in the curvature of the path to be followed. However, the specifics of the path tracking task (all the future curvature is known) allow a predictive principle to be used. This is done for instance in [33], where a future point attached to the path to be followed is tracked instead of the closest point to vehicle position.

The main application targeted in this paper is driver assistance for farm tasks on agricultural machines (such as spraying, harvesting, etc.), since they appear to be tedious for farmers. Automation of driving tasks in agricultural work has been an important centre of interest, especially for vehicle manufacturers. Indeed, such systems are able both to reduce discomfort for the farmer and to increase precision of work achieved, which ultimately reduces pollution. As a consequence, several devices have already been marketed based on different sensors (camera for [9] or laser in [5]) but these are more and more focused on global positioning system (GPS) (see for instance [19]). Even if recent developments enable more phenomena to be taken into account, results do not appear to be satisfactory when sliding occurs. This is particularly so on slopes or when the path to be tracked is a curve.

In this paper, a control law dedicated to an off-road vehicle equipped with a Real Time Kinematic GPS (RTK-GPS – sensor supplying a position accurate to within 2 cm) is developed. The control strategy takes into account not only sliding, but also low level actuators and vehicle inertia. In the first part, a model of sliding (derived from a classical dynamic model) is designed to allow characterization of vehicle lateral dynamics with respect to a reference path (longitudinal motion is not considered in that paper). This model is compatible with a measurement system based on a unique sensor (this approach does not permit the use of a complete dynamic model). As the validity of such an 'extended kinematic model' is confirmed theoretically and experimentally, a new control law is defined to correct behaviour of the vehicle when sliding phenomena are present. Preliminary simulation is then presented and discussed to show the limitations of control methods at the transient moment (when sliding starts to occur). Predictive controls are then investigated and applied to limit this kind of problem. Finally, full scale experiments are discussed and demonstrate improvements in taking sliding into account for accurate guidance of vehicles moving across natural ground. The expected tracking accuracy performance of ± 15 cm is almost always respected in experimental conditions.

2. Vehicle Model With Sliding Taken into Account

2.1. About Dynamic Models

A natural way to take into account sliding phenomena and vehicle inertia in a description of vehicle behaviour, is to investigate dynamic models. As they

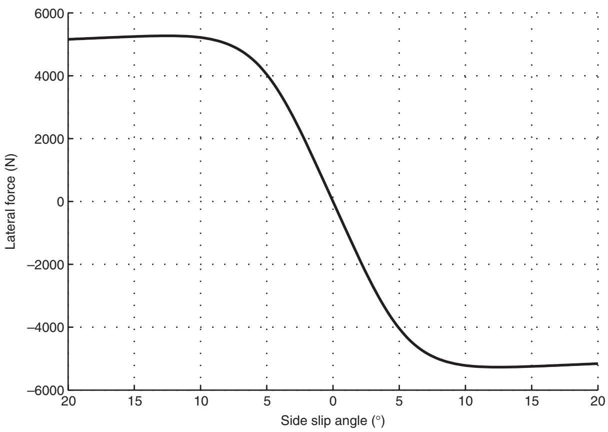

Fig. 1. Relation between lateral forces and side slip angle.

account for many more components (such as inertia or pitch angle and so on ...) than a kinematic description, they appear to be theoretically more accurate. In particular, complex description of tyre/ground contact is modeled, which supplies interaction forces to be applied to the vehicle. As soon as estimations of such forces are available, classical laws of solid mechanics can be applied and lead to dynamic models such as described for example by [21]. Unfortunately tyre models are linked to numerous variables and parameters to be measured or estimated. For example, one of the most celebrated (Pacejka model) – described in [2] – depends on more than 10 parameters to be identified for calculation of lateral forces (and for only one tyre), which are difficult to measure (such as side slip angles and longitudinal sliding rate). As an example of Pacejka formula output, Fig. 1 shows the general shape of the relation between lateral force and side slip angle of a tyre.

Such a chart depends on the following parameters/variables:

- Inertial parameters: inertial moments or matrices, mass distribution on each tyre, etc.
- Geometric parameters: wheelbase, camber, position of centre of gravity, etc.
- Vehicle behaviour variable: longitudinal slip, side slip angle, friction coefficient at tyre/ground contact, etc.
- Tyre parameters (Pacejka for instance), which depend on tyre configuration (pressure, shape, etc).

If some of these variables can be directly measured, parameters of tyre/ground interaction models have to be identified. This is feasible for applications dedicated to cars running on roads (as is done e.g. in [7]), as the nature of the contact does not change significantly. Unfortunately, for off-road applications such as those considered in this paper, these parameters

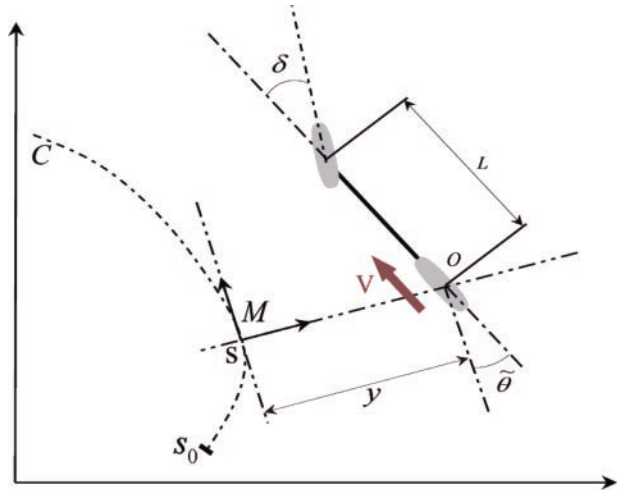

Fig. 2. Classical kinematic model parameters.

vary with respect to adherence properties. Even with tyre/ground interaction models dedicated to off-road vehicles (such as described in [32] or in [12]), on-line estimation of parameters is necessary for the path tracking control application. An important and expensive measurement system is then required, which appears to be hardly practicable.

Approaches based on a complete dynamic model as described for instance in [31] or in [10] appear to be unsuitable with respect to path tracking tasks for off-road vehicles. On the other hand, the use of kinematic models for vehicle control is a convenient and robust approach, which should be preserved as far as possible. As an on-line estimation of some parameters is required for the dynamic model to account for sliding, it seems more relevant to design parameters which can be introduced into a kinematic approach. In this paper, an extended kinematic model is so designed as to provide an accurate description of vehicle behaviour even in the presence of sliding. Control based on such an approach is expected to be more relevant and robust with respect to all-terrain vehicles.

2.2. Extended Kinematic Modeling

2.2.1. Description of Rolling Without Sliding

As our simplified model taking sliding into account takes place on the classical model in rolling without sliding conditions, let us first consider the celebrated Ackermann model. In this approach, the vehicle is reduced to a bicycle shape (as shown in Fig. 2), where the front axle (and similarly the rear axle), which is composed of two wheels, is considered as a single wheel. As the goal of the application is trajectory tracking, description of vehicle evolution is performed with respect to the path to be followed supposedly known to our application (previously computed or stored from a previous run). The absolute state of the vehicle (X and Y position and absolute heading, supplied by system measurement – GPS output) is then turned into a relative position (curvilinear abscissa, lateral deviation and heading deviation). Parameters and notations used in this model are listed below:

- $\mathcal{C}$ is the path to be followed.
- O is the centre of the vehicle's virtual rear wheel.-This is the point to be explicitly controlled.
- M is the point on $\mathcal{C}$ which is the closest to O.

M is assumed to be unique, which is realistic when the vehicle remains quite close to $\mathcal{C}$.

- s is the curvilinear coordinate of point M along $\mathcal{C}$, and $c(s)$ denotes the curvature of $\mathcal{C}$ at that point.
- y and $\tilde{\theta}$ are respectively lateral and angular deviation of the vehicle with respect to the reference path $\mathcal{C}$ (see Fig. 2).
- δ is the virtual front wheel steering angle and the unique control variable.
- v is the vehicle's linear velocity, considered here as a parameter, whose value may be time-varying during the travel of the vehicle. v is assumed to be correctly measured on-line by an appropriate sensor.
- L is the vehicle wheelbase.

With these notations, and assuming in this case that the two virtual wheels (front and rear) of the vehicle are under rolling without sliding conditions, classical system (1) can be calculated:

$$\begin{cases} \dot{s} = \dfrac{v\cos(\tilde{\theta})}{1 - c(s)y} \\ \dot{y} = v\sin(\tilde{\theta}) \\ \dot{\tilde{\theta}} = v\left[\dfrac{\tan(\delta)}{L} - \dfrac{c(s)\cos(\tilde{\theta})}{1 - c(s)\,y}\right] \end{cases} \tag{1}$$

Using this model, a control law without sliding incorporated had been designed in [30] based on chained system theory (detailed in [26]). Represented by Eq. (2), it yields satisfactory results (tracking error remains within a range of ± 15 cm) for trajectory tracking on ground with good adherence properties (such as asphalt). Behaviour can be tuned by the two gains K_p and K_d, consistent with a PD controller.

$$\delta(y,\tilde{\theta}) = \arctan\left(L\left[\frac{cos^3\tilde{\theta}}{(1-yc(s))^2}(-K_d(1-yc(s))\tan\tilde{\theta} - K_p y + c(s)(1-yc(s))\tan^2\tilde{\theta}) + \frac{c(s)\cos\tilde{\theta}}{1-yc(s)}\right]\right) \tag{2}$$

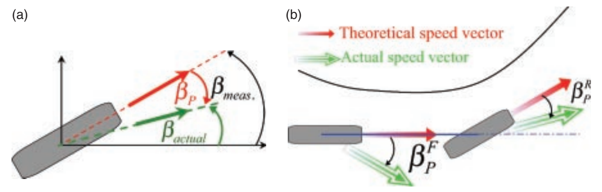

Fig. 3. Sliding parameters to be used in extended kinematic model. (a) Tyre behaviour, (b) Vehicle behaviour.

2.2.2. Sliding Model Description

In this paper, the previous model is extended with some parameters derived from dynamical models. Indeed, in tyre modelling – as can be seen in [2] or in [31] – lateral forces (longitudinal control is not considered in this paper) are calculated mainly with respect to an important dynamic variable: The side slip angle. As shown in Fig. 3(a), the actual speed vector recorded on a tyre is different from the theoretical one, given by tyre's orientation. The difference between this latter direction and the direction of the actual speed vector is hereafter called 'side slip angle' and designated β_P. This angle is mainly responsible for lateral forces and in a dynamic description makes the vehicle turn. This side slip angle is generated both by tyre deformation (corresponding to the linear part of Fig. 1) – the phenomenon is then called pseudo sliding – or by the actual sliding of the tyre on the ground (corresponding to the non-linear part of Fig. 1).

This tyre behaviour can then be introduced into the classical model shown in Fig. 2 and enables the evolution of the vehicle to be calculated using the actual direction of speed vectors. Figure 3(b) defines the new model under consideration, where side slip angles are considered on the bicycle model, one for the front wheel (designated β_P^F) and one for the rear wheel (designated β_P^R). Similar parameters are used by Ackermann in [1] to take account of wind effects on car dynamics.

2.2.3. Kinematic Equations of Movement

A new kinematic model accounting for sliding can then be defined. Notations introduced in Fig. 2 are extended with sliding parameters defined by Fig. 3. The directions of speed vectors used for kinematic calculation then account for sliding parameters β_P^F and β_P^R. This new bicycle model is then consistent with a kinematic model of a vehicle with two steering axles under conditions of rolling without sliding: The front steering angle is $\delta_{Front} = \delta + \beta_P^F$ and the rear one is $\delta_{Rear} = \beta_P^R$. The equations of motion of such vehicles can be calculated in a classical way (see for instance

[18]). The resulting extended kinematic model accounting for sliding proposed in this paper can then be shown to be:

$$\begin{cases} \dot{s} = \dfrac{v\cos(\tilde{\theta} + \beta_P^R)}{1 - c(s)y} \\ \dot{y} = v\sin(\tilde{\theta} + \beta_P^R) \\ \dot{\tilde{\theta}} = v\left[\cos\beta_P^R \dfrac{\tan(\delta + \beta_P^F) - \tan\beta_P^R}{L} - \dfrac{c(s)\cos(\tilde{\theta} + \beta_P^R)}{1 - c(s)y}\right] \end{cases} \tag{3}$$

Naturally, equations of this model are not linear. Nevertheless, as has been pointed out previously, the system (3) looks like a model for a vehicle with two steering axles under conditions of rolling without sliding. Such a consideration is very interesting for the control to be designed on this model, as control of such mobile robots is well known and transformation into an almost linear form (chained system) can be achieved. These results are applied hereafter to the design of the control law associated to model (3). Finally, it can be verified that the classical kinematic model for a vehicle in pure rolling conditions can be deduced from (3): by applying null sliding parameters ($\beta_P^F = 0, \beta_P^R = 0$), the extended kinematic model does indeed become (1).

To use such an extended model, and to achieve the comparison with an actual vehicle, the state variables $(s, y, \tilde{\theta})$ must be measured, but the two sliding parameters (β_P^F, β_P^R) must be evaluated too. The vehicle used for experimental applications must then be equipped with suitable sensors for convenient access to estimates of variables and model parameters.

3. Parameter Observation

3.1. Experimental Context

The vehicle used for experimentation is an Ares 640 tractor lent by the German manufacturer CLAAS, with whom a research partnership has been concluded. It is shown in Fig. 4. The hydraulic drive has been modified to enable automatic steering. To achieve closed loop control of the low level part (steering angle δ), an angle sensor has been installed to measure actual steering angle. This low level closed loop ensures convergence of actual steering angle towards the angle desired, supplied by the control law and sent to the actuator.

The only exteroceptive sensor used to ensure trajectory tracking of this farm tractor is a real time kinematic GPS (RTK GPS), which supplies position information with ± 2 cm accuracy. Use of this material enables direct measurement of state variables (s, y), while vehicle heading (and therefore angular deviation $\tilde{\theta}$) is

Fig. 4. Vehicle used for experimentation.

estimated via a Kalman filter. Consequently, all variables of the state vector are available. Furthermore, the RTK GPS supplies also the antenna velocity, considered as a satisfactory measure of the vehicle linear velocity v introduced in the previous section.

3.2. Direct Measurement of Sliding

On the contrary, the sliding parameters defined in the previous section cannot be directly measured. However, considering the last two equations of model (3) and the information supplied by the sensors, it can be observed that using numerical derivation of measured variables $(y, \tilde{\theta})$, two equations are then available to provide these two unknowns. This 2-dimensional system can be resolved, and finally (β_P^R, β_P^F) can be calculated via Eq. (4):

$$\begin{cases} \beta_P^R = \arcsin\left\{\dfrac{\dot{y}}{v}\right\} - \tilde{\theta} \\ \beta_P^F = \arctan\left\{\dfrac{L}{v\cos\beta_P^R}\dot{\theta} + \tan\beta_P^R\right\} - \delta \end{cases} \tag{4}$$

Even if such sliding estimation leads to acceptable values with respect to expected precision (see for instance [16]), this method is subject to important limitations: firstly, introduction of numeric derivation $(\dot{y}, \dot{\theta})$ of measured variables leads to a very noisy signal. Secondly, delays present in heading signal generate bias in sliding estimation. To overcome these problems, a more convenient on-line sliding estimation based on observer theory has been designed.

3.3. Duality Between Control and Observation

One possible way of evaluating unmeasured variables or parameters of a model is to use an observation algorithm, as described for instance in [4]. It is achieved e.g. with respect to mobile robots in [8] for velocity estimation or in [27] for estimation of side slip angles. In these two references, observers are based on a dynamic vehicle model for passenger car applications. Moreover, more and different kinds of sensors are used than for our application (off-road vehicles). For both the observers cited, unmeasured data are variables included in the state vector. More precisely, vehicle model can be written as eq. (5).

$$\begin{cases} \dot{X} = f(X,u) \\ Y = h(X) \end{cases} \tag{5}$$

For such a system, X is a state vector with a dimension n, while Y is the output with a dimension m such as $m \leq n$. u is a control vector, and finally f and h are functions, which can be non-linear. Considering this system, a classical observer can be defined by eq. (6), where $\hat{X}$ is the observed state vector.

$$\dot{\hat{X}} = f(\hat{X},u) + \phi(Y - h(\hat{X})) \tag{6}$$

On the assumption of observability, an error function is introduced to make estimated output converge with measured output using unmeasured variables. Unknown variables thus calculated are then assumed to be consistent with the actual values. In [27], several kinds of function for ϕ have been tested. Use of such equations could be transposed to our model if sliding parameters were in the state vector X, which is not the case in the formalism of our model (3). It could not be rewritten under such a form, since the derivations of these sliding parameters ($\dot{\beta}_P^F$ and $\dot{\beta}_P^R$) are unknown.

Thus, assuming that the observation problem can be viewed as a dual control problem (which is generally assumed in the literature), observation of sliding parameters is henceforth transposed to a control problem. According to a control description, model (3) is viewed as a process to be controlled with respect to sliding parameters, in order that the state vector converges with measured variables. The following notations and equivalences with respect to control theory are then achieved:

- $u = \left[\beta_P^R, \beta_P^F\right]$ is viewed as control vector of process (3).
- δ: Steering angle. In the following equations, δ is viewed as a measured parameter supplied by the angle sensor fitted on the vehicle steering actuator.
- $\hat{X} = [\hat{y}, \hat{\tilde{\theta}}]$: the state of the observer. In this case, it constitutes the state vector to be controlled.
- $\bar{X} = [\bar{y}, \bar{\tilde{\theta}}]$: the measured vector (output of sensor). This vector is the desired position for the process.

The observer can be synthesized under a classical control approach. The objective is to make state vector $\hat{X}$ (observed state) converge with the target value $\bar{X}$ (measured state) using the control variables $[\beta_P^R, \beta_P^F]$.

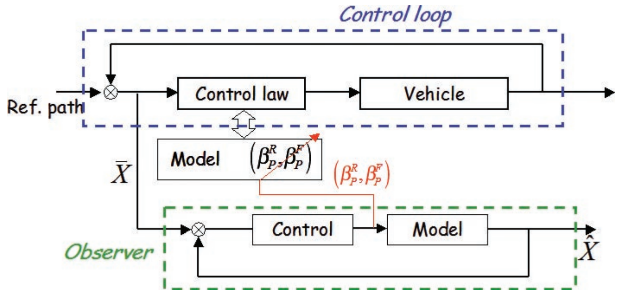

Fig. 5. Main controller and observer loops.

Figure 5 depicts the global algorithm principle, where two loops are running simultaneously. First, the observer loop (at the bottom of the figure) receives input of the measured state vector $\bar{X} = \left[\bar{y}, \bar{\tilde{\theta}}\right]$, which is introduced as the desired state to be reached by observed state $\hat{X} = \left[\hat{y}, \hat{\tilde{\theta}}\right]$. This loop provides estimation of sliding parameters, which is injected into the model, and will be used in the vehicle control loop with sliding incorporated (at the top of Fig. 5, and detailed later in this paper). All required parameters and variables are then available for control design.

3.4. Observer Design

3.4.1. System Formalism

Model (3), with no equation for curvilinear abscissa evolution, is rewritten into a non-linear state representation given by (7):

$$\dot{\hat{X}} = f(\hat{X},u) \tag{7}$$

where f is defined by (3) and is recalled in (8):

$$f(\hat{X},u) = \begin{cases} f_1 = v \sin(\hat{\tilde{\theta}} + \beta_P^R) \\ f_2 = v \left[\cos \beta_P^R \dfrac{\tan(\delta + \beta_P^F) - \tan \beta_P^R}{L} \right. \\ \qquad \left. - c(s) \dfrac{\cos(\hat{\tilde{\theta}} + \beta_P^R)}{1 - c(s)\hat{y}} \right] \end{cases} \tag{8}$$

To control system (7) with respect to sliding parameters, let us linearize this state equation with respect to ‘control vector’ u around zero (no sliding), as side slip angles are close within a few degrees. This leads to eq. (9):

$$\dot{\hat{X}} = f(\hat{X},0) + B(\hat{X})u \tag{9}$$

with $B(\hat{X})$ denoting the derivation of $f(\hat{X},u)$ with respect to control u (sliding parameters), defined by (10)

$$B(\hat{X}) = \frac{\partial f}{\partial u}(\hat{X},0) = \begin{bmatrix} v\cos\hat{\tilde{\theta}} & 0 \\ v\dfrac{c(s)\sin\hat{\tilde{\theta}}}{1-c(s)\hat{y}} - \dfrac{v}{L} & \dfrac{v}{L}\left(1+\tan^2\delta\right) \end{bmatrix} \tag{10}$$

According to definition (10), matrix $B(\hat{X})$ is invertible under the condition: $\tilde{\theta} \neq \frac{\pi}{2}[\pi]$, which is the case during tracking if initialization is achieved correctly.

Convergence of $\hat{X}$ to $\bar{X}$ is ensured if and only if error tends towards zero (hereafter called ε and defined by $\epsilon = \hat{X} - \bar{X}$). As a consequence, an equation defining error dynamics $\dot{\epsilon}$ must be found. However, it requires derivation of $\bar{X}$ (measured state vector), which is not analytically available. Indeed, analytical derivation of $\bar{X}$ defined by (11) cannot be resolved, since the sliding parameters are not estimated yet. Therefore, relation (11) cannot be introduced into the desired error dynamics equation.

$$\dot{\bar{X}} = f(\bar{X},u) \tag{11}$$

A first solution can be to consider a quasi-static evolution of the measured signal (i.e. $\dot{\bar{X}} = 0$), which leads to an equation of error equal to state eq. (9): $\dot{\epsilon} = \dot{\hat{X}}$. Unfortunately, such an assumption is not valid since the evolution of observed state $\hat{X}$ cannot be faster than the evolution of measured state $\bar{X}$. As a consequence, sliding estimation is slightly delayed and therefore an overall control law that relies on such estimation can be unstable.

To overcome this problem, evolution of the measured state vector is introduced into the error equation using its numerical derivation defined by (12), where T is the sampling period.

$$\dot{\bar{X}}^M = \begin{cases} \dfrac{\bar{y}_{[k]} - \bar{y}_{[k-1]}}{T} \\ \dfrac{\bar{\tilde{\theta}}_{[k]} - \bar{\tilde{\theta}}_{[k-1]}}{T} \end{cases} \tag{12}$$

The measured state vector can then be introduced into the error evolution equation. Impact of noise generated by numeric derivation is less important than for eq. (4), since the settling time of the observer will naturally smooth this noisy signal. Error dynamics can then be defined by Eq. (13):

$$\dot{\epsilon} = f(\hat{X},0) - \dot{\bar{X}}^M + B(\hat{X})u \tag{13}$$

3.4.2. *Observer Equations*

The objective of the observer is to make the error ε tend towards zero. This can be ensured by introducing a Hurwitz matrix K and imposing the following condition:

$$\dot{\epsilon} = K \cdot \epsilon \tag{14}$$

On the assumption that matrix $B(\hat{X})$ is invertible, which is true in practical cases (see definition (10)), condition (14) can be ensured by the control law (15) with respect to sliding parameters.

$$u = B(\hat{X})^{-1}\left(K \cdot \epsilon - f(\hat{X},0) + \dot{\bar{X}}^M\right) \tag{15}$$

Relation (15) is an equation for the estimation of sliding parameters, which can be used instead of Eq. (4). The dynamics of convergence for error ε can be tuned by the choice of matrix K, which defines settling time for the observed state. This makes it possible to act on two points which are important for our application:

- Confidence in each measured variable: choice of matrix K allows each settling time to be tuned separately for state variables y (lateral deviation) and $\tilde{\theta}$ (angular deviation). As a result, a longer settling time can be chosen for less certain measured variables. In our case, heading measured by GPS (and then angular deviation) is derived from a Kalman filter, which may not always be relevant. The choice to be made on matrix K will then reduce settling time relative to measured lateral deviation with respect to settling time relative to measured angular deviation. Relevance of sliding parameters is then expected to be improved, quite independently of the time delay present on vehicle heading estimation.
- Noise level on estimated sliding parameters: observer settling time permits smoothing of the observed state with respect to that measured. Consequently, control variables calculated (i.e. estimated sliding) are smoothed in the same way. This effect is limited, however, as settling time must be sufficient to preserve adequate convergence.

3.5. Validation of Observer and Extended Model

3.5.1. *Vehicle Behaviour Under Control with Sliding Neglected*

To demonstrate the capabilities of both model (3) and estimation algorithm (15), let us introduce the results of path tracking obtained under control law (2), when sliding phenomena are neglected. This will make it possible to show the effect of sliding phenomena with respect to the tracking task (referenced to the path to be followed) and to compare actual results with model output. First, let us consider a reference path, during the following of which sliding will inevitably appear. Shown in Fig. 6, it consists of two straight lines separated by a significant curve (half turn) executed on an even field (damp soil, with low adherence properties). The tracking task is performed at an almost constant speed of $9\,\mathrm{km.H}^{-1}$.

The effect of sliding can be viewed in Fig. 7, where the actual tracking error during path following is shown by a black solid line, with respect to the curvilinear abscissa. It may be observed that during the half turn (between curvilinear abscissa 25 m to about 50 m), control law (2) is not able to make the vehicle reach a null lateral deviation: non-negligible sliding effects observed during the curve make the vehicle converge towards an almost constant tracking error of about 30 cm (which is out of the acceptable range expected by the farmer). A significant overshoot of 70 cm is also recorded at beginning of the curve (at curvilinear abscissa 33 m).

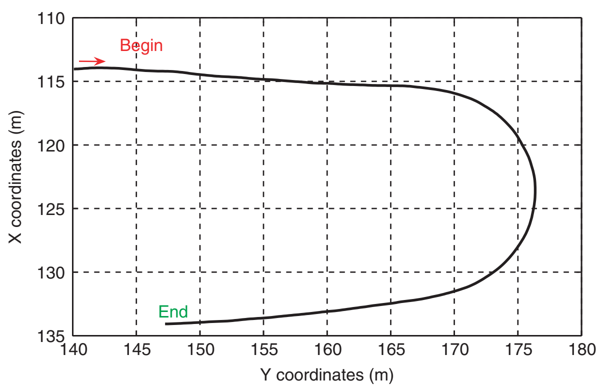

Fig. 6. Reference path to be followed for estimation validation.

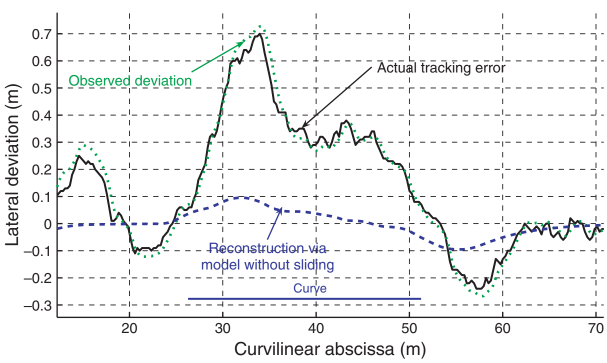

Fig. 7. Tracking error during curve following without sliding incorporated.

The lateral deviation resulting from a simulation using the same control law (2) and using the model without sliding (1) is also shown in this figure by a blue dotted line. This simulation incorporates the low level properties (steering actuator), which explains the overshoots observed at the beginning and end of the curve (when steering angle as to change). During the curve, the model that neglects sliding supplies an almost null lateral deviation, while actual lateral deviation is close to 30 cm. As a consequence, lateral deviation observed for actual vehicles cannot be characterized by model (1), on which the classical control law is based. Logically, control law (2) is not able to deal with this phenomenon, which explains the loss of accuracy during the curve.

3.5.2. Convergence of Observer

During experiments, the matrix K (which determines the convergence rate of the observer) was set to:

$$K = \begin{bmatrix} -1.4 & 0 \\ 0 & -0.8 \end{bmatrix} \tag{16}$$

These values have been experimentally determined to ensure good observer convergence with satisfactory smoothing of sliding parameters and independence of sliding estimation with respect to the delay recorded on vehicle heading. The observed lateral deviation ($\hat{y}$) obtained with such settings during above discussed experiments is shown by a green dotted line in Fig. 7.

It can be seen that this signal accurately fits the actual deviation recorded during path following. This demonstrates the validity of the observer (described by Eq. (15)) with respect to the objective defined (convergence of observer state with measured state). The algorithm is then able to calculate relevant values for sliding parameters to ensure a null error of observation.

3.5.3. Capabilities of Model and Observer

The relevance of estimated parameters with respect to the model (3) can now be checked. Validation is achieved using a simulation based on model (3) (with sliding incorporated) submitted to control law (2) (without sliding incorporated). Simulation results must be superposed on the actual results if the extended kinematic model appears to be adapted to the characterization of vehicle behaviour.

In Fig. 8, results of simulations are compared to actual lateral deviation (still shown as a black solid line). Simulated lateral deviation with the extended model including observer input is shown by a red

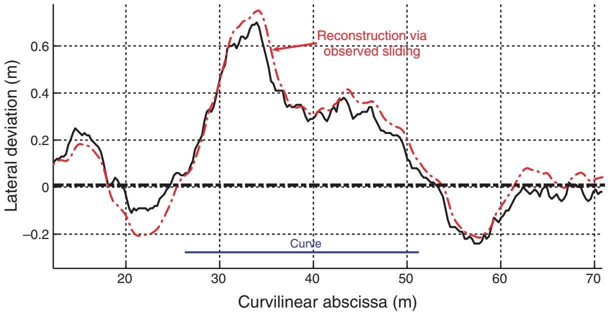

Fig. 8. Results of reconstruction with extended model.

dash-dotted line. The simulation is very close to the actual lateral deviation, and consequently provides a suitable characterization of vehicle behaviour in presence of sliding. The model with estimation algorithm appears to be relevant and constitutes an accurate tool.

4. Control Without Prediction

In this section, a control principle and associated equations are developed. As a consequence, only the theoretical capabilities are demonstrated (experimental tests are presented at the end of paper).

4.1. Chained System Transformation

In this paper, control is based on the extended kinematic model defined by (3), where sliding undergone by the vehicle is integrated as parametric variables. These sliding parameters (i.e. β_P^F and β_P^R) are estimated on-line using observer method (15), as described earlier in this paper. As has been done in previous work (see for instance [15] and [30], in which another model for sliding is proposed), a complete adaptive scheme can be designed to steer a vehicle in sliding conditions, and then enables tracking accuracy to be preserved even in sliding conditions.

Another approach is here favoured, in view of the similarity of model (3) with classical mobile robots models. Indeed, as has been pointed out, model (3) is consistent with the model of a mobile robot with two steering axles moving without sliding. Such a model is known to be transformable into a three dimensional state chained system form with two inputs (see [26]):

$$\begin{cases} \dot{a}_1 = m_1 \\ \dot{a}_2 = a_3\, m_1 \\ \dot{a}_3 = m_2 \end{cases} \tag{17}$$

with $A=(a_1,\ a_2,\ a_3)^T$ and $M=(m_1,\ m_2)^T$ respectively the state and the control vector. In order to reveal that the major part of system (17) is linear, let us replace time derivation by derivation with respect to the first state variable a_1. On the assumption that $m_1 \neq 0$, the following notation can be used:

$$\frac{d}{da_1} a_i = a_i' \quad \text{and} \quad m_3 = \frac{m_2}{m_1} \tag{18}$$

Under these notations, system (17) can be rewritten as follows:

$$\begin{cases} a_1' = 1 \\ a_2' = a_3 \\ a_3' = m_3 = \dfrac{m_2}{m_1} \end{cases} \tag{19}$$

The last 2 equations of system (19) constitute a linear system.

As pointed out in [26], conversion of system (3) into chained forms (17) and (19) can be achieved by introducing the state transformation (20) and the control transformation (21).

$$\Theta(s,y,\tilde{\theta}) = \left(s, y, \tan(\tilde{\theta}+\beta_P^R)[1-c(s)y]\right)^T \tag{20}$$

$$M(s,y,\tilde{\theta},\delta,v) = (m_1,m_2)^T \tag{21}$$

with

$$\begin{cases} m_1 = \dfrac{v\cos(\tilde{\theta}+\beta_P^R)}{1-c(s)y} \\ m_2 = -c(s)v\sin\left(\tilde{\theta}+\beta_P^R\right)\tan\left(\tilde{\theta}+\beta_P^R\right) + v\dfrac{1-c(s)y}{\cos^2(\tilde{\theta}+\beta_P^R)}\left[\cos\beta_P^R\left(\dfrac{\tan(\delta+\beta_P^F)-\tan\beta_P^R}{L}\right)\right. \\ \qquad\qquad \left. -\dfrac{c(s)\cos(\tilde{\theta}+\beta_P^R)}{1-c(s)y}\right] \end{cases} \tag{22}$$

According to system (17), auxiliary control m_2 consists in the time derivative of a_3. Therefore, in view of Eq. (20), an explicit expression of m_2 requires the derivation of the rear sliding parameter, which is not available analytically. As β_P^R is a noisy signal, the use of its numeric derivation does not appear to be very tractable. As a consequence, the expression (22) has been obtained under the assumption that rear sliding parameter β_P^R is slow-varying ($\frac{d}{dt}\beta_P^R \approx 0$).

The conditions of existence and inversion of transformations (20) and (21) are: $y \neq \frac{1}{c(s)}$ (model singularity), $v \neq 0$ (satisfied in the applications considered here) and $(\tilde{\theta} + \beta_P^R) \neq \frac{\pi}{2}[\pi]$ (which is always true in practice, when path tracking is properly initialized).

4.2. Control Law Design

As we are able to turn the kinematic vehicle model into linear form (19), a control law achieving path tracking can be easily designed. Indeed, a natural expression to make the vehicle tend to a null lateral deviation is:

$$m_3 = -K_d a_3 - K_p a_2 \quad (K_p, K_d) \in \Re^{+2} \tag{23}$$

since injecting (23) into system (19) leads to:

$$a_2'' + K_d a_2' + K_p a_2 = 0 \tag{24}$$

Differential Eq. (24) implies convergence to zero of the two variables a_2 and a_3. On one hand, the convergence of a_2 ensures convergence of lateral deviation y. Path tracking is then achieved by the vehicle. On the other hand, $a_3 \rightarrow 0$ is equivalent to $(\tilde{\theta} + \beta_P^R) \rightarrow 0$, which ensures that vehicle heading will compensate the effect of sliding due to rear side slip angle (the vehicle moves crabwise). Sliding due to the front side slip angle will be compensated directly by steering angle, as described by the steering control law expression (25).

In expression (24), the two gains (K_p, K_d) are consistent with gains used in a PD controller. As error dynamics is expressed with respect to a_1, which is equal to the curvilinear abscissa s, these two gains do not specify a settling time, but a settling distance, so that the capabilities of this control law are theoretically independent of vehicle velocity v.

Finally, inversion of the transformation (21) yields an analytic expression for the control law (injecting (23) in (18) and (22)):

$$\delta = \arctan\left\{ \frac{L}{\cos\beta_P^R}\left[C(s)\frac{\cos\tilde{\theta}_2}{\alpha} + A\frac{\cos^3\tilde{\theta}_2}{\alpha^2} \right] + \tan\beta_P^R \right\} - \beta_P^F$$

$$\text{with} \quad \begin{cases} \tilde{\theta}_2 = \tilde{\theta} + \beta_P^R \\ \alpha = 1 - c(s)y \\ A = -K_d\alpha\tan\tilde{\theta}_2 - K_p y + c(s)\alpha\tan^2\tilde{\theta}_2 \end{cases} \tag{25}$$

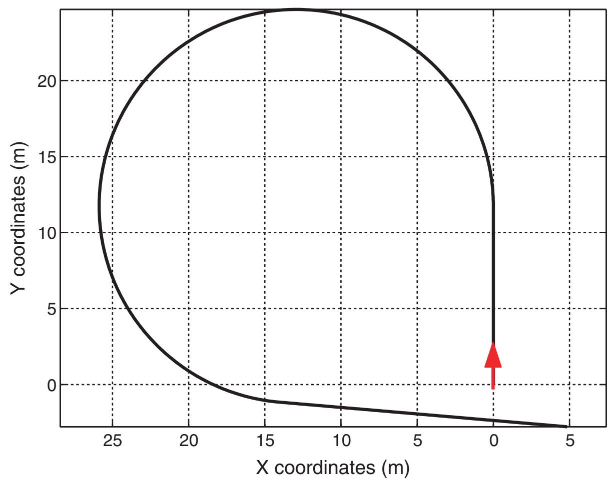

Fig. 9. Theoretical path to be followed.

Eq. (25) constitutes calculation of the steering angle to be sent to the actuator. It can be verified that applying null sliding parameters $(\beta_P^F, \beta_P^R) = (0,0)$ supplies expression (2), which constitutes the previous control law without sliding incorporated, described in [29]. Both control laws (25) and (2) are calculated under the experimental assumption that the terms attached to curvature derivation are negligible.

4.3. Theoretical Results

As the new control law accounting for sliding effects has been designed previously, its theoretical behaviour (convergence to zero when sliding occurs) is checked under simulation and compared to the behaviour obtained with control law (3) which does not account for sliding.

Simulation results deal with the theoretical path to be followed defined in Fig. 9. It is composed of two straight lines linked by a perfect arc of a circle. A curvature step is then introduced at the beginning/end of the circle, which is not compatible with the actuator features (low level properties do not allow the vehicle to follow a curvature step perfectly). Therefore, in order to be more realistic, the simulator takes into account the low level properties of the steering angle actuator: the control applied on the simulated vehicle is linked to the calculated steering angle by a pure delay of 200 ms and a classical second order process with a settling time of 400 ms and a first overshoot of 10%. Sliding parameters are simulated during the curve by defining a proportional relation between side slip angles and steering angle. Finally, during simulation, the vehicle is running at a constant speed of 9 km.H^{-1}.

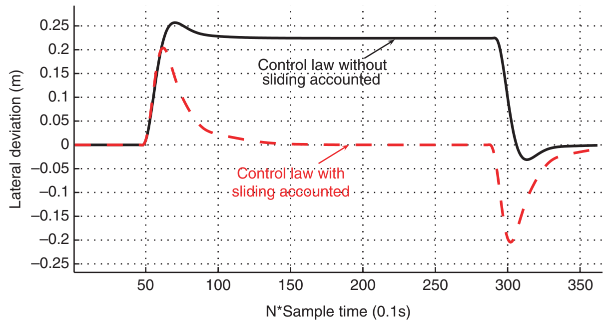

Fig. 10. Comparison of path tracking result with control laws (25) vs. (2).

For both control laws, the same gain values are entered, i.e. $(K_P, K_d) = (0.09, 0.6)$. The lateral deviation obtained with control (25) (when sliding parameters are estimated by the observer defined by (15)) is shown by a red dashed line on Fig. 10, and compared to the tracking error obtained with control law (2), still shown in black solid line.

According to simulation results, the classical control law (without sliding incorporated) makes the vehicle tend towards a constant lateral deviation during the curve (stabilization around 28 cm), while, as expected with regard to Eq. (24), the control law (25) with sliding incorporated causes the vehicle to converge exactly to a null lateral deviation. Thus the model based control strategy as defined by (25) and with on-line observer algorithm input appears to be theoretically a suitable way to preserve tracking accuracy from sliding effects, at least when sliding conditions are constant.

As the simulator takes low level properties into account, Fig. 10 shows overshoots on lateral deviation using control law (25) as soon as sliding appears or disappears (transient phases). These overshoots (linked in simulation to low level response) are amplified in full scale experiments, mainly due to dynamic phenomena and especially to delay induced by vehicle inertia which is not yet taken into account. A solution for delay compensation is presented in the next section.

5. Predictive Control

As abrupt variations of curvature are responsible for transient phases and considering that we know in advance the exact shape of the path to be followed, one way to limit these transient phases is to use a predictive action. Indeed, using such information, it is possible to send a control value to the actuator a moment before the curve appears. Then, the steering angle actually applied to the vehicle when the curve starts could correspond to the desired one and could prevent overshoots due to delays. In this paper, model predictive control is developed.

5.1. Separation of Control Law

Since angular and lateral deviations and especially sliding parameters cannot be anticipated, prediction has to be applied only with respect to curvature. To identify the contribution of curvature in control law (25), let us first assume that the vehicle follows the reference path perfectly. Considering this case and assuming rolling without sliding conditions (since the values of sliding parameters cannot be predicted), the curvature defined by the steering angle of the vehicle has to be equal to the path curvature. This geometrical condition can be analytically described (applying null deviations and sliding in (25)) as:

$$\tan\delta = Lc(s) \tag{26}$$

This consideration reveals a separation into the control law expression. Eq. (25) can be rewritten as follows:

$$\delta = \arctan(u+v) - \beta_P^F$$

$$\text{with} \quad \begin{cases} u = \dfrac{L}{\cos\beta_P^R}\, c(s)\, \dfrac{\cos\tilde{\theta}_2}{\alpha} \\ v = \dfrac{L}{\cos\beta_P^R}\, A\, \dfrac{\cos^3\tilde{\theta}_2}{\alpha^2} + \tan\beta_P^R \end{cases} \tag{27}$$

which can be rewritten under the more convenient expression (28) using the geometrical relation (29):

$$\delta = \delta_{Traj} + \delta_{\mathrm{Deviation}}$$

$$\begin{cases} \delta_{\mathrm{Traj}} = \arctan(u) \\ \delta_{\mathrm{Deviation}} = \arctan\left(\dfrac{v}{1+uv+u^2}\right) - \beta_P^F \end{cases} \tag{28}$$

$$\arctan(a+b) = \arctan(a) + \arctan\left(\frac{b}{1+ab+a^2}\right) \tag{29}$$

Expression of control law (25) under the presentation (28) constitutes the desired separation of the control law into two additive terms, which play two different roles, as detailed below:

- $\delta_{\mathbf{Deviation}}$: Null term when deviations and sliding are equal to zero. This term mainly depends on sliding parameters (β_P^R, β_P^F) and deviations $(y, \tilde{\theta}_2)$ to ensure the convergence of the latter ones to 0. As these variables and parameters cannot be anticipated, this additive term will not be introduced into the predictive algorithm.

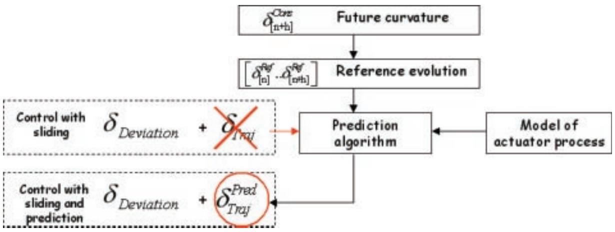

Fig. 11. Application of prediction to control expression.

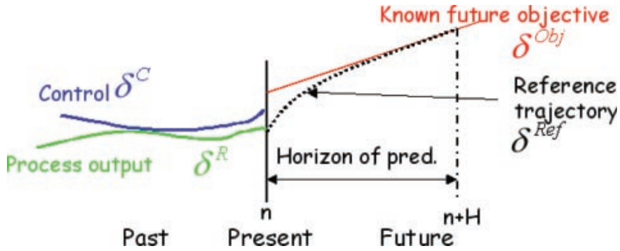

Fig. 12. Notations and general description of PFC.

- $\delta_{\mathbf{Traj}}$: Non-null term when deviations and sliding are equal to zero. This term mainly depends on reference path properties, and ensures path-following condition defined by (26). As the future curvature of the path to be followed is known (attached to the reference path), the future objective attached to this term can be calculated. Model predictive control of this term will be achieved.

5.2. Prediction Algorithm

As soon as the step of control law separation is achieved, the prediction algorithm detailed below is applied to term δ_{Traj} to produce the new term $\delta_{\text{Traj}}^{\text{Pred}}$. As detailed in Fig. 11, the new control law to be sent to the steering actuator is the addition of $\delta_{\text{Deviation}}$ (which remains unchanged) and predictive term $\delta_{\text{Traj}}^{\text{Pred}}$. The Model Predictive Control principle, defined in [23] and applied in [22], forms the basis on which prediction is developed in this section, since the future curvature is known and a model of the actuator is available.

5.2.1. Prediction Principle

The description of predictive functional control (also called model predictive control) requires the definition of the variables shown in Fig. 12 and detailed below:

- δ^C: Control variable sent to the actuator. In the current case of a separate control, this variable is only the trajectory part δ_{Traj} of the control law, defined by (28) and (29).
- δ^R: Measured steering angle. This is the output of low level process resulting from the action of control δ^C, which is only the trajectory part of the control actually applied. As we cannot separate the measured steering angle into two parts, actual response to δ^C is approximated by the relation (30), where $\delta^M_{[n]}$ is the n^{th} measurement of steering angle supplied by the sensor.

$$\delta^R_{[n]} = \delta^M_{[n]} - \delta_{\text{Deviation}[n]} \tag{30}$$

- ***H***: Horizon of prediction. It is the constant time in the future, which will be used to determine the control value to be applied in the present (iteration n) to reach the future objective δ^{Obj} as well as possible. In the remainder of this paper, the integer n_H is the iteration number attached to the horizon of prediction H: n_H defines the number of coincidence points used in prediction algorithm.
- $\delta^{\mathbf{obj}}$: Known future objective. It represents the future desired process output value. In the present case, this variable is linked to the future curvature of the reference path by the relation: $\delta^{\text{Obj}} = \arctan(L.c(s + H_s))$, where H_s is the Horizon of prediction in the curvilinear abscissa associated to H.
- δ^{Ref}: Desired reference shape to be followed by δ^R to reach the future objective δ^{Obj}. This variable determines the desired shape of the process output to converge to δ^{Obj}. Classically, a first order such as relation (31) is chosen, where $i \in [0;n_H]$ and $\alpha \in [0;1[$ is a parameter tuning the convergence speed of reference trajectory.

$$\delta^{\text{Obj}}_{[n+i]} - \delta^{\text{Ref}}_{[n+i]} = \alpha^i \left(\delta^{\text{Obj}}_{[n]} - \delta^R_{[n]} \right) \tag{31}$$

In the current case, only the objective at the moment n_H is used for reference path calculation and is considered as constant all along the horizon of prediction. The reference path is then defined as follows:

$$\delta^{\text{Ref}}_{[n+i]} = \delta^{\text{Obj}}_{[n+n_H]} - \alpha^i \left(\delta^{\text{Obj}}_{[n+n_H]} - \delta^R_{[n]} \right) \tag{32}$$

- $\hat{\delta}^R$: Predicted output of process. This variable describes the evolution of the future process output computed from the identified process model (see next section).

Under these notations, the goal of MPC is to find on the horizon of prediction H, the control set $\delta^C(n, \ldots, n + n_H)$ which minimizes deviation between predicted output $\hat{\delta}^R$ and the desired trajectory δ^{Ref} chosen to reach the final objective $\delta^{\text{Obj}}_{[n+H]}$. A criterion

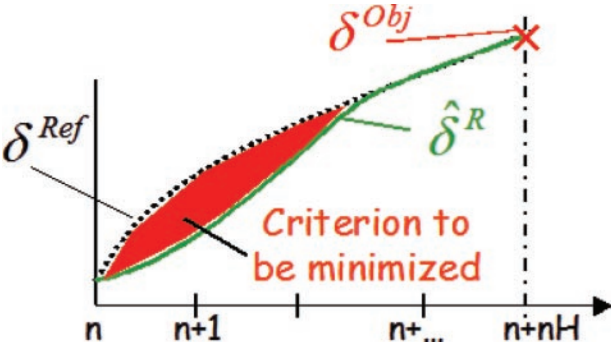

Fig. 13. Visualization of criterion to be minimized.

to be minimized can then be defined. It is shown graphically in Fig. 13, and the mathematical expression of this criterion, hereafter called D, is defined by Eq. (33):

$$D(n) = \Sigma_{i=0}^{n_H}\left(\hat{\delta}^R_{[n+i]} - \delta^{Ref}_{[n+i]}\right)^2 \tag{33}$$

In Eq. (33), the number of coincidence points used for criterion calculation, and consequently for minimization, is equal to the number of iterations required to meet the horizon of prediction. For example, if the horizon is set to 0.9 s, 10 iterations are required, and finally 10 coincidence points are defined.

5.2.2. *Low Level Model*

As calculation of the criterion (and consequently its minimization) requires the prediction of the output of process during the horizon of prediction, a model for the low level actuator must be available. Experiments enable the actuator response to a control input to be measured and an identification establishes that it can be described as second order. As control runs in discrete time, the low level model can be described by model (34):

$$\begin{cases} X^\delta_{[n]} = FX^\delta_{[n-1]} + K\delta^C_{[n-1]} \\ Y^\delta_{[n]} = CX^\delta_{[n]} \end{cases}$$

$$\text{with} \quad X^\delta_{[n]} = \begin{bmatrix} \delta^R_{[n]} \\ \delta^R_{[n-1]} \\ \delta^C_{[n-1]} \end{bmatrix}, \qquad F = \begin{bmatrix} b_1 & b_2 & a_2 \\ 1 & 0 & 0 \\ 0 & 0 & 0 \end{bmatrix},$$

$$K = \begin{bmatrix} a_1 \\ 0 \\ 1 \end{bmatrix}, \qquad Y^\delta_{[n]} = \delta^R_{[n]}, \qquad C = [1 \quad 0 \quad 0] \tag{34}$$

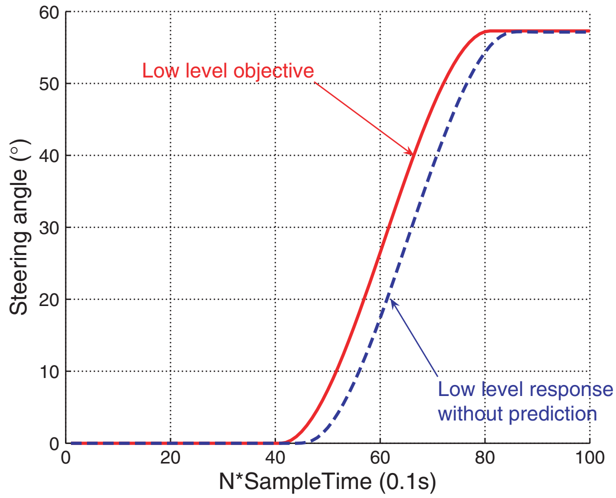

Fig. 14. Low level response to a step.

Model (34) is consistent with the classical form of a discrete second order system. According to experimental tests, the numerical parameters shown in (35) can be deduced, with respect to the sampling time $T = 0.1$ s (10 Hz):

$$\begin{aligned} a_1 &= 0.1237 \quad b_1 = 1.2155 \\ a_2 &= 0.0934 \quad b_2 = -0.4326 \end{aligned} \tag{35}$$

Response of the actuator to a step input can be characterized by the following properties:

- Settling time: 0.5 s
- First overshoot: 3%

Actual response to a classical shape of control input which can be recorded during experiments is presented in Fig. 14.

Here, a pure delay is present, but is taken into account by extending the horizon of prediction. Currently, only the delay due to the actuator process is integrated into the model (34)–(35). However, the influence of other phenomena (filters and vehicle inertia) can be practically reduced by extending the horizon of prediction H and tuning the parameter α used in Eq. (33).

5.2.3. *Prediction Term Calculation*

As a process model is available and knowing the future objective δ^{Obj} derived from (26), minimization of criterion (33) can be developed:

5.2.3.1. Future control structuration. First of all, as future control minimizing $D(n)$ has to be found, a structure composed of base functions must be defined to build it. At a given moment $i \in [0;n_H]$ in the future, a control can be defined, such as:

$$\delta^C_{[n+i]} = \Sigma^{n_B}_{k=1} \mu_k(n) \delta^C_{Bk}(i) \tag{36}$$

In equation (36), δ^C_{Bk} is k^{th} base function chosen, which is time-dependent. The degree n_B of the base set and the shape of base functions δ^C_{Bk}, $k \in [0..n_B]$ depend on the application and on the desired evolution of the future objective. Moreover, as the control which will finally be applied is the first one, i.e. $\delta^C_{[n]} = \Sigma^{n_B}_{k=1} \mu(n) \delta^C_{Bk}(0)$, the set of base functions must be different from 0 when $i = 0$. A classical choice of base functions is $\delta^C_{Bk}(i) = i^{k-1}$, since the first one (i.e. $k = 0$) is amply different from 0 when $i = 0$. Such a structure is chosen in this paper. In the present case, the degree of the base set is limited to 1 (i.e. $n_B = 1$), as discussed in section C. The structure is then finally defined by:

$$\delta^C_{[n]} = \mu_1(n).1 \tag{37}$$

The goal of the minimization problem is now to find the coefficient $\mu(n) = \mu_1(n)$, which will minimize the criterion $D(n)$.

5.2.3.2. Process response. Let us now separate the process response into a free response ${}_L\hat{\delta}^R$ (due to the contribution from previous states and control) and a forced one ${}_F\hat{\delta}^R$ (resulting from the applied control δ^C). Process output can be rewritten as:

$$\hat{\delta}^R_{[n+i]} = {}_L\hat{\delta}^R_{[n+i]} + {}_F\hat{\delta}^R_{[n+i]} \tag{38}$$

On one hand, free response can be easily obtained by recurrence using model (34):

$${}_L\hat{\delta}^R_{[n+i]} = C.F^i.X^\delta_{[n]} \tag{39}$$

On the other hand, the forced response can be defined as follows:

$${}_F\hat{\delta}^R_{[n+i]} = \mu(n) \hat{\delta}^R_B(i) \tag{40}$$

where $\hat{\delta}^R_B$ denotes the forced response to the control δ^C_B and can be explicitly calculated using recurrence equations (34).

5.2.3.3. Minimization of the criterion: Inserting (39), (40) into (38) and injecting the latter into definition of criterion (33), the expression of $D(n)$ becomes:

$$D(n) = \Sigma^{n_H}_{i=0} \left\{ \mu(n) \hat{\delta}^R_B(i) + C.F^i.X^\delta_{[n]} - \delta^{Ref}_{[n+i]} \right\}^2 \tag{41}$$

In expression (41), the unknown variable to be determined is $\mu(n)$. Let us introduce $d(n+i) = \delta^{Ref}_{[n+i]} - C.F^i.X^\delta_{[n]}$. Relation (41) can then be written as:

$$D(n) = \Sigma^{n_H}_{i=0} \left\{ \mu(n) \hat{\delta}^R_B(i) - d(n+i) \right\}^2 \tag{42}$$

Minimization of the criterion can now be obtained by canceling the gradient $\frac{\partial D}{\partial \mu}$, which leads to the relation:

$$\Sigma^{n_H}_{i=0}\, 2\left(\mu(n) \hat{\delta}^R_B(i) - d(n+i) \right) \hat{\delta}^R_B(i) = 0 \tag{43}$$

which is equivalent to:

$$\mu(n) \left(\Sigma^{n_H}_{i=0} \left(\hat{\delta}^R_B(i) \right)^2 \right) - \Sigma^{n_H}_{i=0} \left(d(n+i) \hat{\delta}^R_B(i) \right) = 0 \tag{44}$$

As $\Sigma^{n_H}_{i=0} \left(\hat{\delta}^R_B(i) \right)^2$ is non-null, because it is the sum of positive or null terms with the condition $\hat{\delta}^R_B(0) \neq 0$, $\mu(n)$ can be deduced. Finally, considering that the control to be applied is the first term of the control set (i.e. $i = 0$), according to Eq. (37) the value of the control in the present case is given by:

$$\delta^{Pred}_{Traj} = \delta^C_{[n]} = \mu(n) \tag{45}$$

Lastly, the expression of the trajectory part incorporating prediction to be applied in the control law is given by (46):

$$\delta^{Pred}_{Traj} = \frac{\Sigma^{n_H}_{i=0} \left(d(n+i) \hat{\delta}^R_B(i) \right)}{\Sigma^{n_H}_{i=0} \left(\hat{\delta}^R_B(i) \right)^2} \tag{46}$$

It may be observed that for calculation, the denominator is invariant and can be calculated off-line. The same remark can be made about the calculation of each $\hat{\delta}^R_B(i)$, $i \in [0, \ldots, n_H]$.

5.2.3.4. Global control law expression. Using the result of the criterion minimization presented by (46), the separation equation defined by Eq. (28) and according to the algorithm shown in Fig. 11, we have access to

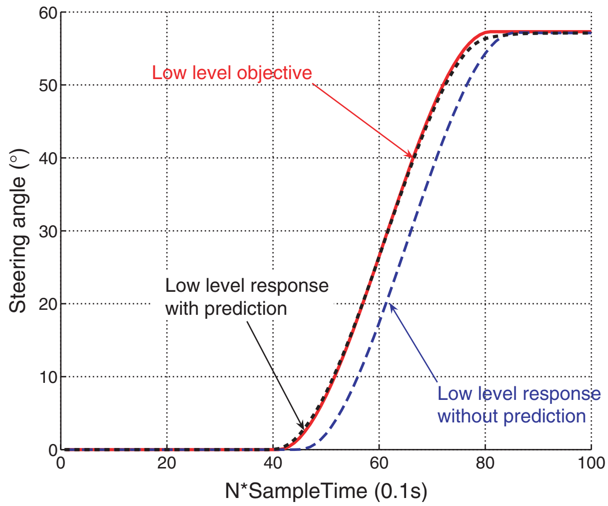

Fig. 15. Result of prediction algorithm.

the whole control law with sliding incorporated and using prediction on the reference path curvature:

$$\delta = \arctan\left(\frac{v}{1+uv+u^2}\right) - \beta_P^F + \frac{\Sigma_{i=0}^{n_H}\left(d(n+i)\hat{\delta}_B^R(i)\right)}{\Sigma_{i=0}^{n_H}\left(\hat{\delta}_B^R(i)\right)^2}$$

$$\text{with} \begin{cases} u = \dfrac{L}{\cos\beta_P^R} c(s) \dfrac{\cos\tilde{\theta}_2}{\alpha} \\ v = \dfrac{L}{\cos\beta_P^R} A \dfrac{\cos^3\tilde{\theta}_2}{\alpha^2} + \tan\beta_P^R \\ \tilde{\theta}_2 = \tilde{\theta} + \beta_P^R \\ \alpha = 1 - c(s)y \\ A = -K_d\alpha\tan\tilde{\theta}_2 - K_p y + c(s)\alpha\tan^2\tilde{\theta}_2 \end{cases} \tag{47}$$

5.3. Theoretical Results with Prediction

5.3.1. Low Level Response with Prediction Algorithm

As a result for predictive algorithm studies (only concerning $\delta_{\mathrm{Traj}}^{\mathrm{Pred}}$), let us consider the same objective evolution δ^{Obj} as described in Fig. 14. Control δ^C defined by (46) – considering that $\delta_{\mathrm{Deviation}}$ is then null – with an horizon of prediction of 0.3 s and a parameter α equal to 0.3 is applied on process model (34) instead of objective δ^{Obj}. The results are presented in Fig. 15 by a black dotted line.

It may be observed that using the prediction algorithm, process output fits the desired objective instead of lagging behind. In this algorithm, at each sample period, a constant objective δ^{Obj} is applied all along the horizon of prediction and the control structure is of degree one, i.e. $n_B = 1$. These facts make the quality of the prediction algorithm sensitive to the choice of the horizon of prediction: If H is too long, control starts too early. This problem could have been eliminated by using actual objectives at each coincidence time and by applying a control structure of degree two, i.e. $n_B = 2$. However, this configuration requires an accurate model for the vehicle response to a steering sequence (in our case, only the actuator is accurately modelled). In contrast, the choice of a degree one in control structure and a constant objective along the horizon of prediction constitute a means of opposing delays due to other phenomena than low level properties, precisely by increasing the horizon of prediction H.

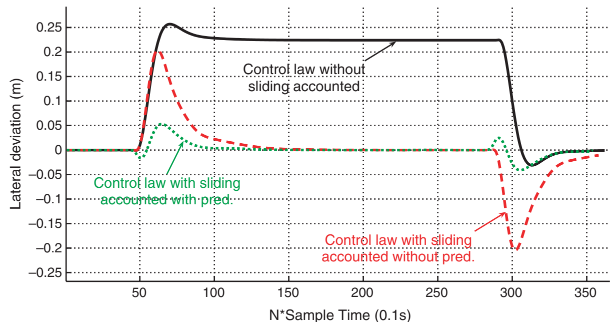

Fig. 16. Result of prediction algorithm on lateral deviation.

5.3.2. Path Tracking using the Prediction Component

As the objective is to reduce the overshoots observed at each beginning/end of curve under control law (25) (cf Fig. 10), let us apply the whole algorithm described by Fig. 11 for vehicle path tracking in the same conditions and on the same trajectory as for the simulation described in Section 4.3. The results of the simulations are reported in Fig. 16.

In addition to the lateral deviation obtained when relying on the classical control law (in solid black line) and on control law (25) (in dashed red line), the path-following result using the algorithm with the predicted trajectory term $\delta_{\mathrm{Traj}}^{\mathrm{Pred}}$ is shown by a dotted green line. The parameters for the prediction are $H = 0.5$ s and $\alpha = 0.2$. The gains used for the deviation part $\delta_{\mathrm{Deviation}}$ remain unchanged for all three control laws, i.e. $K_p = 0.09$ and $K_d = 0.6$.

It may be observed that the overshoots present at each curvature modification (at iterations 50 and 300) are considerably reduced. They are not eliminated, but

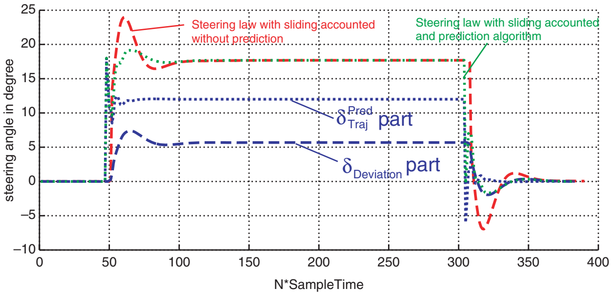

Fig. 17. Comparison of virtual control applied on vehicle.

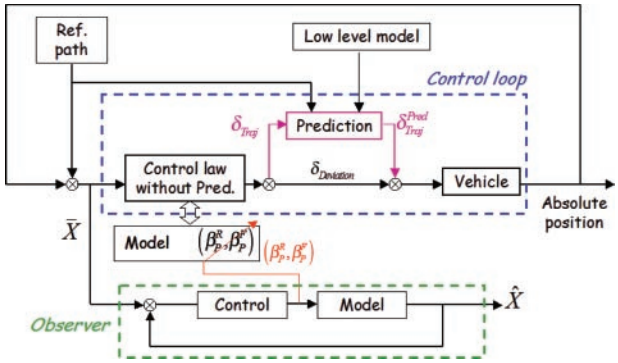

Fig. 18. Complete scheme of control strategy.

it is important to notice that the theoretical path to be followed, shown in Fig. 9, cannot be perfectly followed. Indeed, because of its construction (the circle is linked to two straight lines), a curvature step appears. Since simulated low level cannot accommodate a step in steering angle, overshoots have to be present at each step of curvature.

An important point is that, while curvature on the reference path is constant, the prediction applied on $\delta_{\mathrm{Traj}}^{\mathrm{Pred}}$ does not disturb the convergence of control law term $\delta_{\mathrm{Deviation}}$, which controls the deviations with respect to the path to be followed and compensates effects of sliding. Indeed, after a settling time of about 50 iterations, lateral deviation when using the control law defined by (47) converges perfectly in theory to zero, in the same way as when control law (25) was used.

This can be more precisely observed in Fig. 17, which shows values of steering angles sent to the actuator of the simulated vehicle. The broken red line represents the result of the Eq. (25) (control with sliding incorporated but without prediction) while the dotted green line shows the result of Eq. (47) (control with sliding incorporated and prediction). As expected, the control law with prediction initiates reaction before curvature appears and the values of both control laws during curve remain absolutely unchanged. A breakdown of the evolution of the control incorporating prediction is presented to show both influences of $\delta_{\mathrm{Traj}}^{\mathrm{Pred}}$ (blue dotted line) and of $\delta_{\mathrm{Deviation}}$ (blue dashed line). When following the path shown in Fig. 9, it is clear that the contribution of the trajectory part is more important than that of the deviation part.

In theory, the benefit of predictive strategy at abrupt curvature evolutions is very satisfactory and the same correction capabilities with respect to deviations and sliding parameters are conserved. In practical cases, as described below, similar results can be obtained only if the horizon of prediction is increased (as vehicle inertia increases delay in vehicle reaction). Moreover, in addition to reduction of overshoots, the prediction algorithm has to bring a further benefit in full scale experiments: as the steering wheels will begin to turn before the actual appearance of a curve, they will turn more slowly, and consequently sliding will appear more gradually. This fact favours the hypothesis of slow-varying sliding parameters and the negative effect of filters on sliding estimation will be reduced.

5.4. Overall Scheme of Control

The complete control law defined by (47), with input from observer Eq. (15), constitutes the new control strategy applied instead of Eq. (2). It can be illustrated by the scheme shown in Fig. 18.

The overall control algorithm can be separated into two main loops, one for the observer, and one for effective control (as in Fig. 5). Input into these loops are tracking errors (lateral and angular), extracted by comparison between measured position and orientation and the geometry of the reference path. The observer loop checks the sliding parameters to ensure convergence between the observed and measured states. As sliding is then estimated, the control loop is in possession of all the necessary data and the calculation of control law (25) based on the extended kinematic model, with input from the observer, can be achieved. This control equation is nevertheless separated into two additive terms, namely $\delta_{\mathrm{Deviation}}$ and δ_{Traj} defined by Eqs. (27) and (28). Then, using the future configuration of the path to be followed and a model of the low level actuator, the prediction algorithm summarized by Eq. (46) converts δ_{Traj} to $\delta_{\mathrm{Traj}}^{\mathrm{Pred}}$. Prediction output is added to the deviation part $\delta_{\mathrm{Deviation}}$ in order to obtain the final control law to be applied to the vehicle.

This algorithm constitutes on one hand an observer-based control strategy, derived to access the unmeasured variables required for an accurate control calculation. The extended vehicle model is then on-line adapted to actual behaviour by using observed sliding parameters. On the other hand, a Model Predictive Control is partially applied to the control law to guard the process against inevitable delays which appear during actual experiments due to actuators and non-modeled dynamics.

6. Experimental Results

6.1. Application on an Actual Vehicle

The control strategy defined in this paper is applied on an actual tractor (presented in Section 3.1) for trajectory tracking on fields. The parameter settings cited below are those actually used for all experimental tests presented in this paper:

6.1.1. Control Law Gains

Gain tuning for the new control law defined in this paper is the same as for the control law with sliding ignored. This ensures about the same dynamics as when sliding does not occur (i.e. a settling distance of 15 m without any overshoot). Comparison of the capabilities of all control laws can then be achieved, since differences in performance are not linked to a modification of the theoretical vehicle response.

$$\begin{cases} K_p = 0.09 \\ K_d = 0.6 \end{cases} \tag{48}$$

6.1.2. Observer

The Hurwitz matrix K, which defines the convergence time of observed to measured states is the same as the one defined by (16). It ensures convergence times of 2.1 s for observed lateral deviation and 3.8 s for observed angular deviation. Reminder of the definition of the K matrix:

$$K = \begin{bmatrix} -1.4 & 0 \\ 0 & -0.8 \end{bmatrix} \tag{49}$$

6.1.3. Predictive Control

The parameters of predictive control that are tunable are the horizon of prediction H and the parameter α specifying the convergence rate of the reference trajectory for the low level process. These two parameters have been chosen as follows:

$$\begin{cases} H = 1\ s \\ \alpha = 0.2 \end{cases} \tag{50}$$

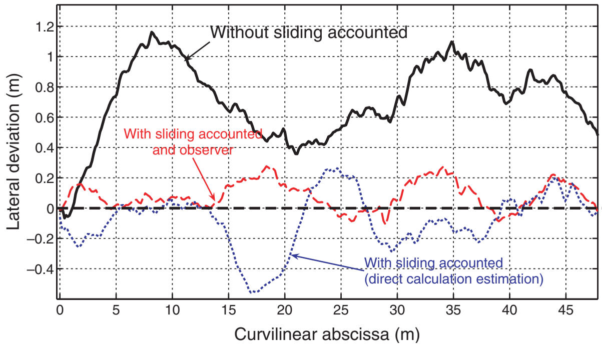

Fig. 19. Comparison of tracking error on a slope with and without observer.

As only the low level model is theoretically entered for the calculation of the prediction term, the horizon of prediction chosen for actual experiments is higher than the theoretical one. This choice is expected to compensate for the neglected delays due to dynamics (and especially for neglected vehicle inertia).

6.2. Results on a Slope

The first case encountered in agricultural tasks, where the sliding phenomenon is very harmful to tracking accuracy, is the following of a straight line on a slope. Generally, the straight line to be followed is perpendicular to the slope. Gravity and low adherence properties lead then to an approximately constant lateral deviation which could be considerable. Hereafter, tests have been carried out on a wet field with an inclination of about 15%. On such terrain, tracking error under control (2) (with sliding ignored), shown by a solid black line in Fig. 19, climbs up to about 1 m.

In the same figure, results of path-tracking carried out at the same speed of about 8 $\mathrm{Km.H}^{-1}$ using control (47) are represented by a red dashed dotted line. As can be observed, the algorithm incorporating sliding makes it possible to keep the tracking error much closer to zero and often within the acceptance range of ± 15 cm. Indeed, the lateral deviation is inside this acceptance range during 75% of tracking time. This value increases to 90% if the range is extended to ± 20 cm. As a comparison, results with sliding neglected show that the tracking error is never within an acceptable range of ± 15 cm during the entire tracking time (except at initial time, but this is not significant).

Such results constitute a considerable improvement, very close to the farmer's expectations. The isolated instances of inaccuracy which can be observed around curvilinear abscissa 18, 34, and 44 m are due to abrupt variations of adherence properties and slope values.

Table 1. Numerical comparison of tracking error

	Mean (cm)	Std. dev. (cm)	Max. dev. (cm)	in ± 15 cm (%)
Without sliding (2)	72	26	114	4
With sliding and obs. (47) + (15)	7	9	28	75
With sliding without obs. (47) + (4)	− 7	19	55	56

They can be observed on the tracking relying on control law (2) as well, as lateral deviation evolves very quickly (e.g. from 60 cm to 1 m just before curvilinear abscissa 34 m). Because prediction is developed on variations attached to an abrupt modification of curvature, it cannot predict variations due to adherence properties or slope.

The numerical comparison proposed in Table 1 confirms the significant improvement when following a straight line on a slope. Statistical data from the lateral deviation signal have been extracted (mean, standard deviation and maximum range of deviation, and finally the percentage of time inside the acceptance range of ± 15 cm). We can notice that the mean value of the tracking error is much closer to zero. The mean value of 7 cm that is recorded is essentially due to the isolated overshoots, as can be verified by the standard deviation value, which is under 10 cm for the new control law. This shows that variability in the tracking error signal is greatly reduced with control law (47). This fact is emphasized by the maximum error value which is reduced by more than 60%.

To go further in the analysis of the algorithm, the last line of Table 1 presents properties of tracking error signal when using the new control (47), but with sliding parameters estimated via direct calculation (i.e. Eq. (4)). This signal is also shown by a dotted blue line in Fig. 19.

This underlines the importance of the sliding estimation algorithm and the capabilities of the observer proposed in this paper. It can be seen that when direct calculation is used, tracking results oscillate much more and accuracy is much less than when using the observer. This follows from the numeric time derivation required in (4) and from the already mentioned lack of confidence in the heading signal.

As a conclusion, accuracy of tracking is very close to farm task requirements in this first case of harsh conditions of mobility. The occasional deviations recorded are then very difficult to compensate, as such very rapid variations of adherence conditions cannot be anticipated.

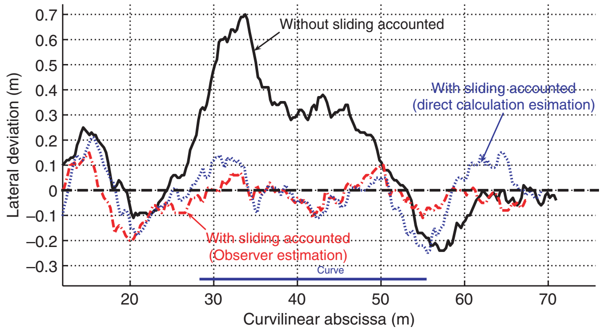

Fig. 20. Tracking error result on half turn.

6.3. Results Relative to Curved Path on Even Ground

The second case of path-tracking where sliding has a very negative effect on accuracy is the following of a curved path on an even ground. The reference trajectory used for the actual experiments has been shown in Fig. 6. As already observed previously, a control law without sliding incorporated cannot achieve satisfactory tracking. This is again displayed in solid black line in Fig. 20: During the curved part of the path, i.e. between curvilinear abscissa 28 m to 55 m, a large lateral deviation can be noticed.

On the same figure, path-tracking results relying on control law (47) are shown by a red dashed dotted line. During the curve, lateral deviation stays very close to zero, instead of permitting a significant deviation, and remains fairly constant. Moreover, overshoots at each transient phase (beginning/end of curve, at 28 and 55 m) can be considered as non-existent, demonstrating the effectiveness of predictive action introduced in Section 5. Accuracy of path tracking is then independent of the shape of the curve to be followed.

This can be corroborated by the numerical properties of the lateral error signal presented in Table 2 (with the same values inserted as before). Tracking error remains within an acceptance range of ± 15 cm during 95% of tracking time and reaches 99% for ± 20 cm. When relying on the control law without sliding incorporated, acceptance ranges ± 15 and ± 20 cm are only met during 48 and 54% of tracking time (since tracking error is close to zero only outside the curved zone). Moreover, when relying on the algorithm presented in this paper, the tracking performance is well centred around the objective of null tracking error: mean value is close to null (-1 cm} against 20 cm for classical control), and variability is very limited (standard deviation of only 5 cm).

Table 2. Numerical comparison of tracking error

	Mean (cm)	Std. dev. (cm)	Max. dev. (cm)	in ± 15 cm (%)
Without sliding	20	25	70	48
With sliding and obs. (47) + (15)	− 1	5	20	95
With sliding without obs. (47) + (4)	− 1	10	25	84

Such results are a little bit better than in the slope case as abrupt variations of sliding are here essentially due to curvature modification and can be compensated via the prediction algorithm (which is not efficient in the slope case). However, reduction of overshoots linked to the prediction algorithm is consolidated by the use of the observer. This can be seen by comparing the results with those obtained when the same control law is used, but sliding parameters are estimated by Eq. (4), cf. blue dotted line in Fig. 20.

Even if mean values of lateral deviation with observer and direct calculation are the same (in both cases tracking error is centered around null value), the variability obtained with direct calculation is much greater (standard deviation is twice that recorded with the use of the observer). This can indeed be explained by investigating transient phases at modification of curvature. Even if prediction is successful in greatly reducing overshoots, delays already pointed out in the slope case reduce the performance of a control law relying on direct calculation (4).

As a conclusion, in the case of path following on even ground, when sliding is essentially induced by the geometry of the trajectory, the algorithm proposed is particularly suitable: the prediction algorithm, associated with a control incorporating sliding via an observer, is here completely efficient, in contrast to the slope case. The tracking algorithm is able to preserve performance whatever the path to be followed and adherence properties. As can be observed, accuracy of tracking is almost independent of sliding and practically always in the acceptance range required for agricultural tasks.

7. Conclusion and Future Work

The overall algorithm presented in this paper shows a high accuracy solution to achieve path-tracking for mobile robots in all-terrain conditions (independent of the shape of the path to be followed and of the adherence properties of the ground on which the vehicle runs). The main negative phenomena which are compensated by the control proposed in this paper are sliding effects and the different delays due to low level actuators and vehicle inertial effects.

As the rolling without sliding assumption cannot be used, an extended kinematic model has been designed, ensuring an accurate description of vehicle evolution including lateral sliding effects, and preserving the advantage of the kinematic approach. The only two variables in this extended new model which cannot be directly measured are the sliding parameters. An observer method is developed to supply the model online with relevant estimates.

Since this extended kinematic model presents similarities with classical mobile robot models, a nonlinear control law can be calculated relying on chained system theory. The capabilities of such control are satisfactory when sliding parameters vary slowly, but are limited by the inevitable delays due to both the steering angle actuator and vehicle inertia. As a result, overshoots appear as soon as a significant variation of curvature must be followed. Even if it only appears in isolation, such a phenomenon is not acceptable, as the tracking error recorded in such cases (e.g. when the vehicle is entering/leaving a curve) can reach quite significant values.

A model predictive control principle has so been developed relying both on reference path geometry and on the available low-level model. It is adapted to the control law with sliding incorporated and enables both anticipation of approaching curvature and compensation for sliding phenomena. The predictive principle is not yet transferred to slope anticipation, as there is no sensor measuring slope integrated into the process. Nevertheless, variations of sliding parameters induced by slope modifications are less abrupt than those generated by curvature changes.

Finally, the capabilities of such an algorithm are demonstrated by full scale experiments on a farm tractor. The application is assistance for drivers of agricultural machineries, inevitably subjected to sliding phenomena, in view of their mass (which may vary according to the implement fitted), and the ground on which they move. The results of the path tracking control law presented in this paper show that tracking accuracy can be preserved whatever the path to be followed and whatever the adherence properties of the ground: the overall algorithm almost always keeps the tracking error within an acceptance range of ± 15 cm, with a very limited variability, meeting then the expectations of farmers. Nevertheless, some points can be improved, essentially with respect to path following on slope, where residual overshoots are still present.

As pointed out in slope experiments, abrupt variations of sliding conditions on such fields can degrade path tracking accuracy in certain instances, mainly because the observation algorithm is submitted to inevitable delays. Extension of estimation to include the high gain principle is therefore under development, to enable observer settling time to adapt to the evolution rate of the measured state. Moreover, as sliding parameters integrated into the extended kinematic model are compatible with a dynamic approach (they are side slip angles), a dynamic model can be used for observer design. The observer can then react faster and other phenomena can be taken into account.

The use of a partially dynamic model is also under investigation for the predictive part. Indeed, vehicle inertia is expected to be integrated into the model used for the predictive algorithm. Prediction will then be based on a more suitable model, so that accuracy can be improved.

Finally, the guidance law presented in this paper relies exclusively on a single RTK-GPS sensor. The results are satisfactory, but although such sensors are becoming cheaper all the time, they are still quite expensive. Extension of the guidance law so that it can rely on several low cost sensors is under study. As a general rule, future work will deal with the addition of sensors and dynamic effects (via partial dynamic models) in order to conserve acceptable accuracy while at the same time reducing costs.

References

1. Ackermann J. Robust lateral and yaw control. In European Summer School in Automatic Control, Grenoble France, 2002
2. Bakker E, Nyborg L, Pacejka HB. Tyre modeling for use in vehicle dynamics studies. In International Congress of the Society of Automotive Engineers (SAE), 1987, pp. 2190–2204
3. Blanc G, Ait Aider O, Mezouar Y, Chateau T, Martinet P. Autonomous image-based navigation in indoor environment. In proceedings of the IFAC/EURON Symposium on Intelligent Autonomous Vehicles 2004, Lisboa, Portugal, 2004
4. Bornard G, Celle-Couenne F, Gilles G. Observability and Observer, Volume 1 of Non-Linear Systems. Chapman and Hall, 1995
5. Brunnert A. Machine guidance with laser and GPS. In Proceedings of the Conference on Crop Harvesting and Processing 2003, Kentucky, USA, 2003
6. Corradini LM, Leo T, Orlando G. Experimental testing of a discrete-time sliding mode controller for trajectory tracking of a wheeled mobile robot in the presence of skidding effects. J Robot Syst 2002; 19(4): 177–188
7. d'Andréa Novel B, Chou H, Ellouze M, Pengov M. An optimal control strategy for a vehicle to brake in corner with stability. In Journées Automatique et Automobile, Bordeaux France, 2001
8. d'Andréa Novel B, Ellouze M. Tracking with stability for a vehicle braking in a corner. In Proceedings of the IEEE Conference on Decision and Control 2001; 5: 4427–4432
9. Debain C, Chateau T, Berducat M, Bonton P, Martinet P. A guidance system for agricultural vehicle. Comput and Electron Agric 2002; 25(1–2): 29–51
10. Dormegnie E, Fandard G, Mahajoub G, Zarka F. Dynamique du véhicule. Technical Report, IFMA, Clermont-Ferrand France, 2002
11. Ellouze M, Andréa-Novel B. Control of unicycle-type robots in the presence of sliding effects with only absolute longitudinal and yaw velocities measurement. Eur J Control 2000; 6: 567–584
12. Harnisch C, Lach B, Jakobs R, Troulis M, Nehls O. A new tyresoil interaction model for vehicle simulation on deformable ground. Veh Syst Dyn 2005; 43: 384–394
13. Hermosillo J, Sekhavat S. Feedback control of a bi-steerable car using flatness application to trajectory tracking. In Proceedings of the American Control Conference 2003; 4: 3567–3572
14. Kim G, Chung W, Kim M, Lee C. Tripodal schematic design of the control architecture for the service robot PSR. In Proceedings of the IEEE International Conference on Robotics and Automation 2003; 2: 2792–2797
15. Lenain R, Cariou C, Thuilot B, Martinet P. Rejection of sliding effects in car like robot control: Application to farm vehicle guidance using a single RTK GPS sensor. In Proceedings of the IEEE International Conference on Intelligent Robots and Systems 2003; 4: 3811–3816
16. Lenain R, Cariou C, Thuilot B, Martinet P. Adaptive and predictive non linear control for sliding vehicle guidance: Application to trajectory tracking of farm vehicles relying on a single RTK GPS. In Proceedings of the IEEE International Conference on Intelligent Robots and Systems 2004, Sendai Japan, pp. 455–460
17. Lindgren DR, Hague T, Probert-Smith PJ, Marchant JA. Relating torque and slip in an odometric model for an autonomous agricultural vehicle. Auton Robots 2002; 13: 73–86
18. Micaelli A, Samson C. Trajectory tracking for unicycle-type and two-steering-wheels mobile robots. INRIA research report 2097, 1993
19. O'Connor M, Elkaim G, Bell T, Parkinson B. Automatic steering of a farm vehicle using GPS. In Proceedings of the International Conference on precision agriculture 1991, Mineapolis, USA, 1996, pp.767–777
20. Peynot T, Lacroix S. Enhanced locomotion control for a planetary rover. In Proceedings of the IEEE International Conference on Intelligent Robots and Systems 2000; 1: 311–316
21. Pham M. Modélisation mathématique du comportement dynamique d'une automobile dans le domaine non-linéaire. Rev Soci Ing Automob, 40, 1986
22. Richalet J. Industrial applications of model based predictive control. Autom 1993; 29: 1251–1274

23. Richalet J. Pratique de la Commande Prédictive. Traité des Nouvelles Technologies Série Automatique. Hermés, Paris, 1993
24. Richard JP. Time-delay systems: an overview of some recent advances and open problems. Autom 2003; 39: 1667
25. Rivals I. Modelling and control of an autonomous vehicle using neural networks. Méc ind matér 1999; 52(1): 10–12
26. Samson C. Control of chained system. IEEE Trans Autom Control 1995; 40: 64–77
27. Stephant J, Charara A, Meizel D. Experimental evaluation of side slip angle. In Proceedings of the IEEE Intelligent Vehicles Symposium (IAV) 2004, Lisboa, Portugal, 2004, pp. 150–155
28. Thuilot B, Bom J, Marmoiton F, Martinet P. Accurate automatic guidance of an urban electric vehicle relying on a kinematic GPS sensor. In Proceedings of the International Symposium on Intelligent Autonomous Vehicles (IAV) 2004, Lisboa, Portugal
29. Thuilot B, Cariou C, Martinet P, Berducat M. Automatic guidance of a farm vehicle relying on a single CP-GPS. Auton Robots 2002; 13: 53–71
30. Thuilot B, Lenain R, Martinet P, Cariou C. Accurate GPS-based guidance of agricultural vehicles operating on slippery grounds, Focus on Robotics and Intelligent Systems Research: Liu Jx (Ed.), Nova Science publisher, 2006
31. Wong JY. Some recent developments in vehicle-terrain interaction studies. J Terramechanics 1991; 28(4): 269–288
32. Zhang Q, Qiu H. A dynamic path search algorithm for tractor automatic navigation. Trans Am Soc Agric Eng 2004; 47(2): 639–646